Organization of Ruthenium(II) and Osmium(II) Complexes in 2-Dimensions Using Self-Assembled Cyclic DNA Nanostructure

Mohamed A. Elnaas[1], Hanadi F. Sleiman[2]
[1]Department of Chemistry, Misurata University, Misurata, Libya
[2]Department of Chemistry, McGill University and Center for self-Assembled Chemical Structures

Abstract:

we have shown that a new DNA nano-square motif can be used to precisely position ruthenium and osmium complexes at the corner of self-assembled DNA square. The strategy used in this work was based on DNA strands conjugated at the end of DNA strands, where the transition metal-DNA conjugates were used to hybridize with the complementary sequences of already assembled DNA nano-square motif.

This methodology is used to assemble hetero-polynuclear metals on this DNA square, where ruthenium and osmium complexes are positioned in a corner of square according to the base pairing of transition metal-DNA conjugates. The metal-DNA assembly is studied using PAGE and FRET experiments. Quenching of the ruthenium emission of up to 35% is obtained as result of the DNA self-assembly. Simply by choosing the right components (number of bases, DNA sequences, site of conjugation, metal ions, and peripheral ligands we can control the size of the self-assembled DNA, and the distance between the chromophores. This can lead to applications in nanooptics and light-harvesting and diagnosis.

Key words: DNA Nanotechnology, Nanoscience, Selfassembly, luminescence, transition metals, DNA synthesis

Introduction:

Photoinduced energy transfer between chromophore (donor, **D**) and quencher (acceptor, **A**) in polynuclear complexes has been the subject of intense investigation.[1-3] There are two reasons for this interest. The first is to understand and mimic the photosynthesis process, which takes place naturally in plants by harvesting the energy of sunlight through complex steps of energy-transfer and electron-transfer.[4,5] The second is to explore the use of photoinduced energy transfer in non-natural systems, for possible applications in molecular electronics and molecular sensing.[6-9] The challenge of designing a system capable of promoting directed energy transfer is to find the proper linker between the donor and the acceptor.[1] This linker is used as bridge between the chromophores, and it has a significant role in controlling the distance and the orientation between them. The linker also affects also the mechanism of the energy transfer between the donor and acceptor.[2,6]

The precise and predictable positioning of small molecules on the nanometer scale (10^{-9} m) has currently attracted significant attention.[11] Self-assembly of molecular components is an attractive strategy in the construction of materials and devices on the nanoscale.[12-14] A successful bottom-up self-assembly approach to such nanomaterials has been demonstrated using different types of interactions, such as

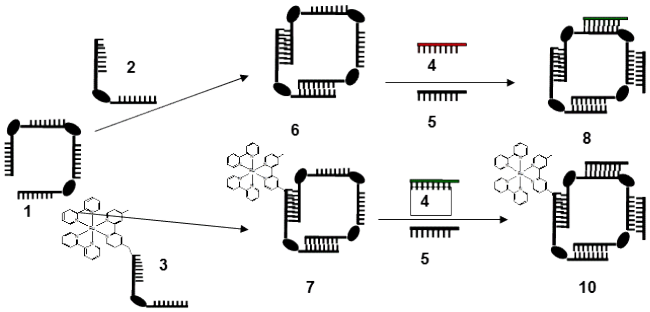

Scheme 1. Self-assembly of DNA building blocks. Squares **8** and **10** formation via the self assembly of DNA building blocks **1**

hydrogen-bonding, metal coordination chemistry, electrostatic and ionic interactions and Van der Waals forces, metal coordination chemistry.[15] Due to its features, DNA has been recognized as a useful and efficient building scaffold in the assembly of nanomaterials.[16] The advantages of DNA have been exemplified in the self-assembly of various artificial nanostructures in two and three dimensions to form periodically patterned arrays and mechanical devices.[16-18] In addition, DNA self-assembled scaffolds have been utilized in the organization of functional groups such as proteins,[19,20] nanoparticles,[21-25] and various small molecules.[26-32] Self-assembled DNA structures functionalized with materials was accomplished using a number of methods. One of these uses a "sticky-end" approach, where the 2D-DNA scaffold is equipped with short DNA strands coming out from its plane, allowing for functionalization with materials that have DNA strands complementary to these sticky-ends.[16] This method generates flexible immobilized materials, limiting the control of distance between neighboring molecules. A second method involves the incorporation of these materials within the self-assembled DNA structure, which is accomplished by using these molecules as vertices and/or linkers. This method provides more control of the distance between the functional materials, however this approach would remove any dynamic character for these structures, and attempts to remove or modify the functional material can result in the collapse of the whole structure. It is highly desirable to develop new methods where the functionalized molecules could be accurately fixed within the DNA assembly in two dimensions with the option to remove, displace or modify them using external stimuli. Recently Sleiman and Aldaye reported the assembly of discrete cyclic square and triangle nanostructures made of single stranded oligonucleotides. These nanostructure were assembled using enzymatic ligation, and proved to be useful in the organization of gold nanoparticles in a precise and predictable manner.[22]

Molecular assemblies containing ruthenium and osmium complexes have been constructed using bridging ligands,[10] polymers,[33] dendimers,[34] hydrogen bonding,[35] intercalation,[36] and attachment to a DNA linear duplex.[37-39] Tor and co-workers have

studied photoinduced energy transfer from a ruthenium complex to an osmium complex attached to ds-DNA.[40] There are very few reports of supramolecular self-assembled structures containing different metal complexes.[41]

Here we report the controlled positioning of ruthenium and osmium complexes in two dimensions. This is accomplished through the self-assembly of a small DNA discrete square structure possessing functional groups (transition metal complexes) that are addressable using light or redox processes. The square structure was assembled using two building blocks consisting of DNA strands possessing bipyridyl (bpy) molecules, embedded as the vertices within the DNA construct (Scheme 1). Building block **1** contains four single strands (8 nucleotides in length) separated by three bipyridine

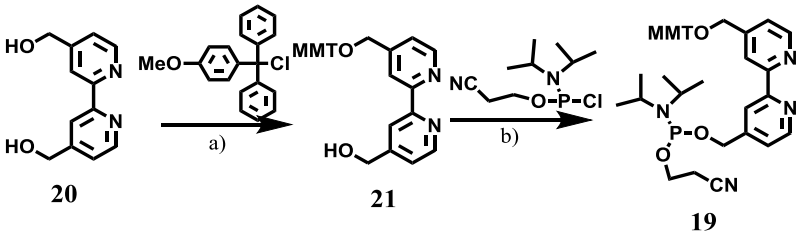

Scheme 2. Synthesis of the asymmetric bipyridine ligand **4.19**. a) CH_2Cl_2, Et_3N, 50%.; b) CH_2Cl_2, iPr_2EtN, 95%

molecules which represent the three corners of the square. The terminal strands of building block **1** are designed to be complementary to **2** or **3**, which is equipped with two single strands (8 nucleotides in length) separated by one bpy (the fourth corner of the square). Subsequent cyclization of **1** occurs upon association to **2** or **3**, to afford DNA squares (**6 or 7)** exhibiting four bipyridine vertices that may be used for further functionalization.[27,29,42] These cyclic nanostructures possess two single strands. Addition of complementary oligonucleotides tagged with ruthenium or osmium complexes results in the positioning of the two transiting metal complexes in close proximity to promote energy transfer from $Ru(bpy)_3^{2+}$ (donor) to $Os(bpy)_3^{2+}$ (acceptor) complexes.

Results and Discussion:

For the synthesis of bipyridine incorporated oligonucleotides, an asymmetric bipyridyl ligand **19** compatible with automated DNA synthesis was prepared. The bipyridine ligand **20** is selected as a vertex for two reasons; the first reason is the directionality of the two hydroxyl groups which would orient the two attached oligonucleotides at about 70° angles.[27] Such an angle would orient the two DNA strands in way that insures the formation of square with defined structure. The second reason is the ability of the two nitrogens on the ligand to coordinate to a large number of metals which would allow for the generation of extended arrays upon the reaction of bpy-DNA squares with transition metals.[29] Scheme 4.2 shows the synthesis of a monoprotected bipyridine phosphoramidite **19** (see Experimental Section). First, reaction of the dihydroxy-bipyridine **20** with one equivalent of the protecting group (MMT-Cl) afforded the mono-protected ligand **21** in 50% yield. Phosphitylation of the second hydroxyl group affords the activated bipyridine amidite **19** in excellent

yield (95% yield). This bipyridine-amidite **19** was characterized using ^{1}H, ^{13}C, ^{31}P NMR, and mass spectroscopy. Using this asymmetric molecule during automated DNA synthesis would allow the incorporation of bipyridine ligand at a desired position in the backbone of DNA strand. Additionally, as a result of this divergent approach two asymmetric DNA strands can be conjugated to the bipyridine ligand at the same time. DNA-bpy conjugates **1** and **2** were synthesized using standard DNA protocols (Scheme 4), through the site-specific incorporation of the modified bpy monomer **19** during solid-phase synthesis. The first DNA strand was initially grown by coupling eight nucleotides on the solid support in a 3'-5' direction, followed by the introduction of the bipyridine amidite **19** to afford the intermediate **23**, which was oxidized, and deprotected to give **24**. The chain is extended from the bipyridine vertex to the desired length of the building block through incorporation of subsequent nucleotides to **25**. Similarly, another bipyridine ligand can be added until the desired number of ligands and DNA strands is reached. The building blocks were cleaved from the support, deprotected, isolated and purified according to standard DNA protocols (see Experimental Section).

The isolated compounds were analyzed using denaturing polyacrylamide gel electrophoresis (PAGE) (Figure 1), giving rise to slow electrophoretic mobility as a function of charge, conformation and sequence type. Analysis of the modified

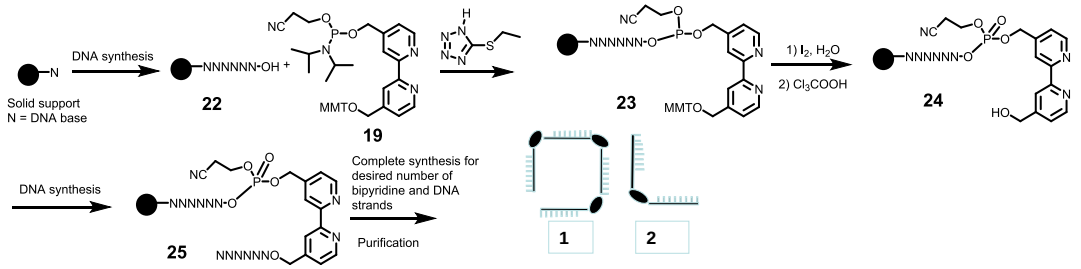

Scheme 3. Automated DNA synthesis of Building **1** and **2**

oligonucleotides by MALDI-TOF mass spectrometry resulted in the expected molecular weights with high purity (see Experimental Section).

Self-Assembly of the DNA square:

The self assembly behavior was analyzed by nondenaturing PAGE (Scheme 1

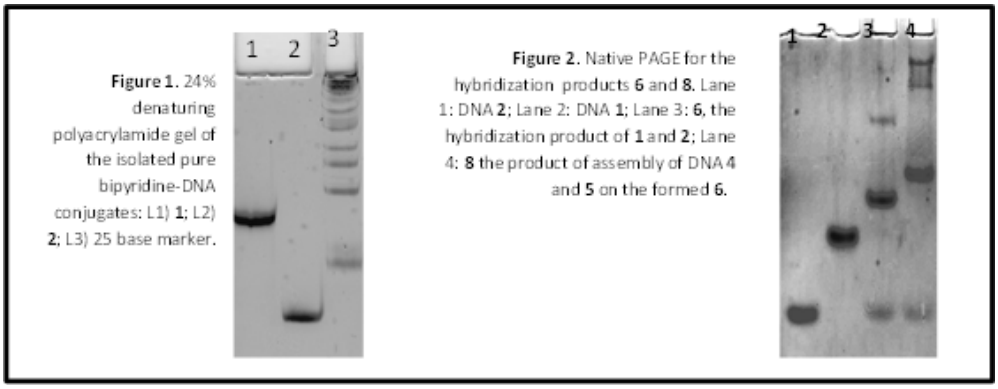

Figure 1. 24% denaturing polyacrylamide gel of the isolated pure bipyridine-DNA conjugates: L1) **1**; L2) **2**; L3) 25 base marker.

Figure 2. Native PAGE for the hybridization products **6** and **8**. Lane 1: DNA **2**; Lane 2: DNA **1**; Lane 3: **6**, the hybridization product of **1** and **2**; Lane 4: **8** the product of assembly of DNA 4 and **5** on the formed **6**.

(top) and Figure 2 lane 3), whereby building blocks **1** and **2** were combined in equimolar amounts at low temperature (<10 °C). The resultant almost exclusive formation of a square structure was observed. This square (**6** in Scheme 1) contains two single strands, two rigid double strands, and four bipyridyl molecules as relatively rigid vertices. Interestingly, only very small quantity of higher molecular weight structures are formed, indicating preference of intramolecular hybridization and cyclization. This is in contrast to many previously reported double stranded DNA

systems, in which polymeric products in addition to cyclic structures form upon hybridization. [23,27,31] It is most likely the result of conformational mobility imparted by the single stranded portion of the molecule **1**, which can relieve any strain resulting from cyclization. A shift in mobility is observed upon addition of **4** and **5**, as evidenced by the formation of the fully double stranded square (**8** in scheme 1**)**. The band in lane 4 of the native gel (Figure 2) shows the formation of a major product corresponding to the fully double stranded DNA square **8** along with a minor product corresponding to the octamer structure. The formation of this higher-ordered structure is likely due to the dissociation of two **8** molecules and their reassociation to form the cyclic octamer. Preliminary modeling shows that the asymmetric square **8** has a cavity of about ~ 2.5 nm, with ~ 2.7 nm long double stranded DNA arms. The vertex, $bpy(PO_3)_2$, is ~ 1.3 nm long, which contribute to the square's overall size. Each corner of the assembled nanostructure is different from the rest in terms of internal distance and relative orientation. In order to estimate the distance between the donor and the acceptor the helical nature of double-stranded DNA has to be considered. The length of right-handed B-DNA increases by 3.4 Å for each base pair is added, and according to this estimation DNA double strand has a length of 20 Å. For this reason, the distance between two chromophores would depend on the number of base pairs and their respective positions around the cylindrical DNA backbone.[43]

To confirm cyclic structure of **8**, an enzymatic digestion study using Mung Bean nuclease (MBN) was carried out. MBN selectively digests single-stranded DNA (ssDNA) over double-stranded DNA dsDNA. Following optimization, the fully dsDNA square structure **8** and ssDNA building block **1** as control experiment, were subjected to enzymatic digestion. While the self assembled structure was not degraded by the enzyme after incubation for 3 hrs (lane 3), building block **1** was completely degraded (Figure 3). If the hybridization product of **1** and **2** was not cyclic, i.e. contains two single strands, this would result in partial degradation of the assembled product upon treatment with MBN, and this new product would move faster in polyacrylamide gel comparing to the one untreated with the enzyme. The results show no change in mobility upon treatment with MBN due to its resistance to the enzyme activity, consisting with the cyclic nature of **8**.

Functionalization of the Square. We used ruthenium and osmium –DNA conjugates to demonstrate the feasibility of **6** and **7** as templates in the assembly of small molecules in a predictable manner. It is noteworthy that there are eight sites on the

DNA (four building blocks, each with 3′ and 5’ positions on their ends) suitable for attaching functional molecules, as well as four bipyridine ligands that may be addressable through coordination with transition metals, and this could be used to further label DNA structures. Ruthenium and osmium complexes were used as functional groups due to stability and compatibility with DNA chemistry as well as their inherent photophysical properties. Ruthenium and osmium complexes are luminescent, redox active, and are similar in structure. It is also well established that osmium complexes quench the excited state of ruthenium complexes when they are positioned in close proximity.[10,33,35] We chose to use 8 base-long oligonucleotides to attain a short distance between the corner of the squares, in order to facilitate resonance energy transfer between ruthenium and osmium complexes formed upon self-assembly. It was reported in the literature that similar ruthenium and osmium complexes have R_0 of 20 Å,[35] where R_0, the critical Förster radius, is the distance at which 50% of the donor’s excited-state energy is transferred to the acceptor. Shorter DNA strands would render the DNA assembly unstable at room temperature. On the other hand longer DNA strands would result in a distance between the two complexes too large for efficient RET to occur.

Generally, end-functionalization of DNA is accomplished by reaction of the unprotected hydroxyl group on the DNA strand with the phosphoramidite derivative of the molecule to be conjugated. Due to the instability of the phosphoramidite derivatives of ruthenium and osmium complexes, we have taken advantage of automated DNA solid-phase synthesis by adopting a reverse coupling protocol

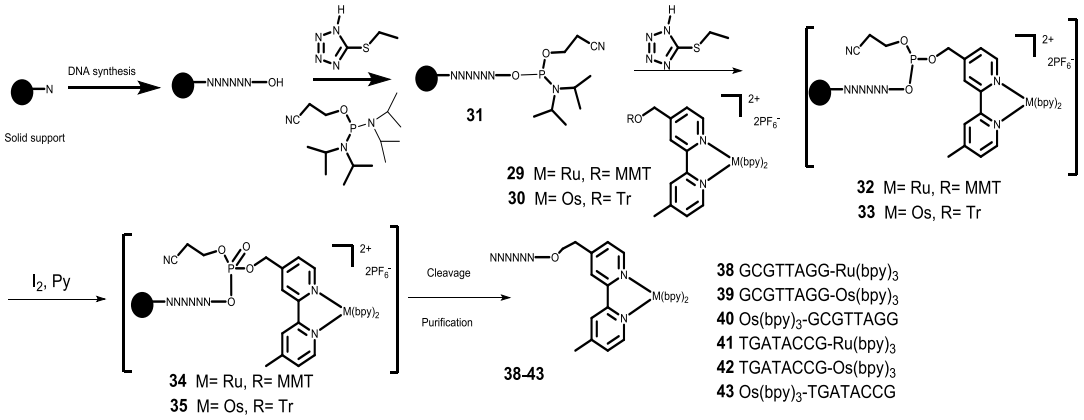

Scheme 3. Conjugation of metal complex to DNA. Synthesis of metal-DNA building blocks **38**-**43**.

reported previously (see Scheme 4).[44] For this purpose ruthenium **29** and osmium **30** complexes functionalized with one hydroxyl group were synthesized following literature procedures from bipyridyl-methyl hydroxyl and $Ru(bpy)_2Cl_2$ **27** and $Os(bpy)_2Cl_2$ **28** respectively.[33]

In the synthesis of ruthenium or osmium DNA conjugates (Scheme 4), oligonucleotide was grown on the solid support using either conventional (3′-5′) or reverse (5′-3′) coupling protocol. The hydroxyl group on the last base is deprotected

and then activated by phosphitylation using (2-cyanoethyl)bis(diisopropylamino) phosphine to give **31**. In order to prevent intermolecular coupling between adjacent oligonucleotides, an excess reagent (50 fold) and a low density (1000 Å LCAA-CPG support with a loading density of (28 μmol/g) solid support were used. After washing the solid support, the metal complex equipped with the hydroxyl group is allowed to react with the activated DNA strand in the presence of the activating reagent, 5-ethylthiotetrazole, to induce bond formation between the transition metal complex and DNA to give the DNA-metal complex **32** and **33** for ruthenium and osmium complexes respectively. After washing, oxidation, the conjugates **34** and **35** are cleaved and deprotected using standard DNA chemistry. The products are purified using PAGE and sephadex. Using this method seven metal-oligonucleotide conjugates were synthesized **7** and **38-43** (Scheme 4). The DNA conjugates were characterized using UV-vis, luminescence, mass spectrometry, and gel electrophoresis. The ruthenium and osmium complexes display typical UV-vis absorbance at 450 nm and 488 nm, respectively along with absorbance peaks between 260 and 300 nm. These electronic transitions in the visible range are characterized as metal to ligand charge transfer bands (MLCT). Higher energy absorptions with a larger extinction coefficient appear between 260 and 300 nm, originating from the DNA bases and the bpy ligands. The DNA-ruthenium conjugates spectrum show a maximum at 260 nm and a shoulder at

Around 280 nm. The oligonucleotides labeled with osmium show a peak at high energy with two maxima at 260 nm and 280 nm, attributed to the absorption of DNA bases and bpy ligands respectively.

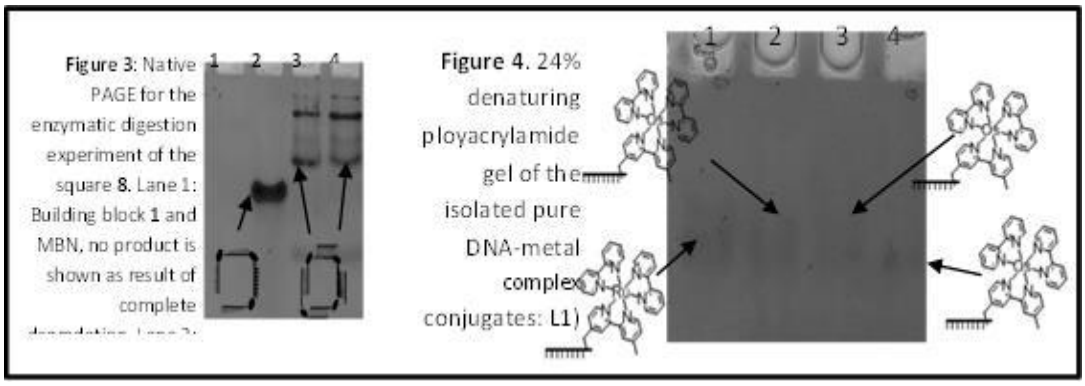

The luminescence in the Ru-DNA complex is retained, showing an emission peak centered at 600 nm upon irradiation of the ruthenium-DNA using light at 450 nm (see emission peak of **3** in Figure 7 a and b).

All the transition-metal oligonucleotides were Characterized By Gel electrophoresis, exhibiting slower

Electrophoretic Mobility compared to that of unconjugated DNA (8 bases) As Control (Observed using
UV light shadowing or staining) (Figure 4).

This large retardation is due to the additional molecular weight of the complex and the +2 positive charges on the transition metal center. The metal-DNA conjugate bands could also be detected as colored red bands under natural light on the gel. The successful conjugation of DNA metal complex was further confirmed by MALDI-TOF mass spectrometry (see Experimental Section).

Following conjugation of ruthenium and osmium complexes to oligonucleotides, the Ru- and Os-DNA conjugates may assemble along the template scaffold of **6** through Watson-Crick base-pairing. The assembly of the conjugated nucleotides on this square was analyzed using PAGE experiments and luminescence quenching studies. The square was first assembled by combining building blocks **1** and **2**, followed by sequential addition of the desired complementary transition metal-oligonucleotide at

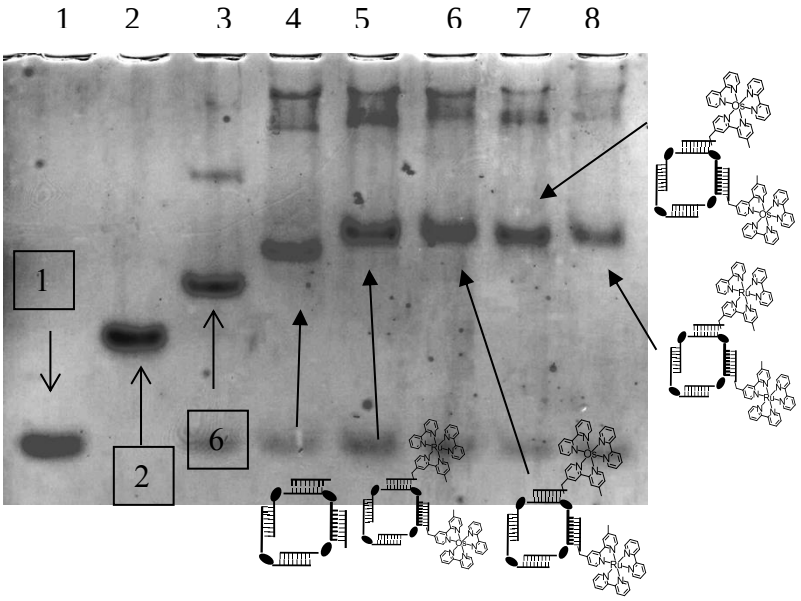

Figure 5. Native PAGE analysis: Hybridization study of metal-DNA conjugates to metal containing squares. Lane 1: **2**; Lane 2: **1**; Lane3: **6**; Lane 4: **8**; Lane 5: **12**; Lane 6: **11**; Lane 7: **13**; Lane 8: **14**. See scheme 1 and figure 1 fo more clear square structures.

low temperature (<10 °C). Figure 5 shows the resultant specific binding of DNA conjugates. In the case of two metal-DNA conjugates of the same type addition, the fully hybridized squares **13** and **14** (lane 7 and 8) run slightly slower than the **8** control (lane 4) as a result of the positive charge and molecular weight of the transition metal complex. Moreover the DNA nanostructure **6** can be addressed by two different metal-oligonucleotides to produce the bimetallic DNA structures **11** and **12** (L5 and L6 in figure 5).

Another experiment was conducted using building blocks **1** and **3** (Scheme 1). This assembly results in the formation of discrete square structure (**7**, Scheme 1) containing a ruthenium complex as well as two single strands. This functionalized assembly **7** is capable of positioning DNA- metal complex conjugates resulting in the formation of nano-scaled squares with one, two, or three transition metals organized

around the cyclic structures in predictable manner. The control positing of the osmium complex in two dimensions with respect to the ruthenium complex attached to the square nanostructure **7** can be accomplished using different osmium-DNA conjugates. Four osmium-oligonucleotides **39**, **40**, **42**, and **43** were assembled on the

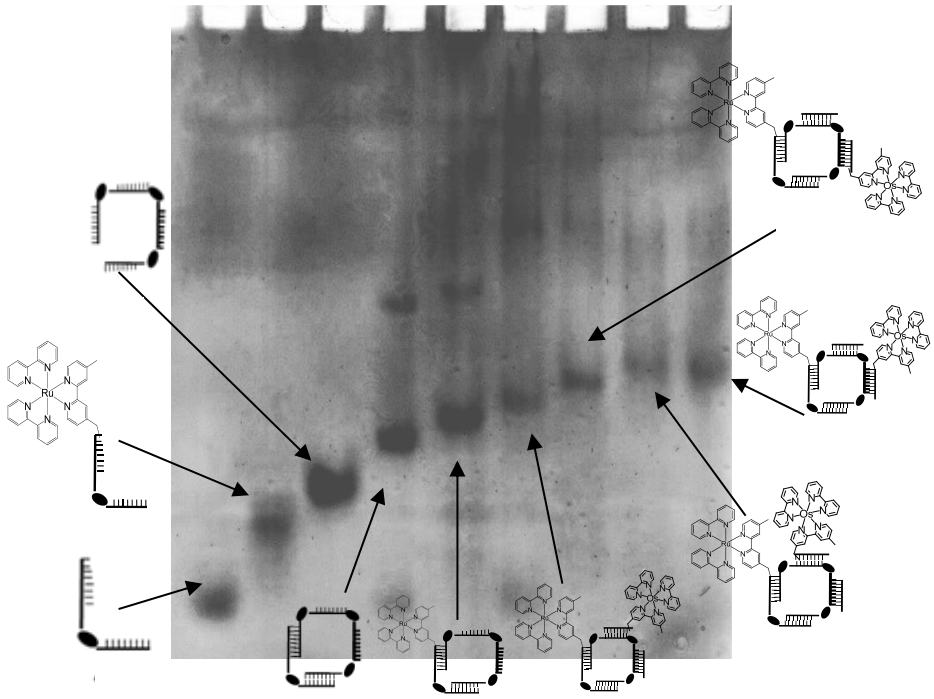

Figure 6. Native 10% TAE PAGE for the assembly of squares containing multi-metals. Lane 1: **2**; Lane 2: **3**; Lane 3: **1**; Lane 4: **6**; Lane 5: **7**; Lane 6: **15**; Lane 7:**16**; Lane 8: **17**; Lane 9: **18**. See scheme 1 and figure 1 for clear view of square structures.

preformed nano-square **7** to give the bimetallic-DNA square structures **15-18** (Figure 6). These metal-DNA squares have the same DNA sequences and one ruthenium complex and one osmium complex; however they are different regioisomers, where each square has the osmium complex in different places with respect to the ruthenium complex. This variation on the structure of the assembled metal-DNA squares is the result of the place of attachment of the osmium complex to DNA, either 5' or 3', and the sequence of the DNA strands. These bimetallic DNA nanostructures were analyzed using PAGE, in L2 the band corresponded to ruthenium-DNA conjugate **3** showed slower mobility than the unmetalized one **2**. Similarly, the metalated square **7** (L5) travels in the gel slower than square **6** (L4) as result of the weight and the charge of the ruthenium complex. The fully hybridized bimetallic-DNA square structures **15-18** travel slower than the square **7** (Figure 6). To our knowledge, this constitutes the highest level of modularity in the positioning of transition metal complexes in self-assembled structures.

These DNA square nanostructures containing ruthenium and osmium complexes were also characterized by fluorescence fluorescence spectra to detect whether fluorescence resonance energy transfer (FRET) was occurring. This phenomenon occurs when two dyes (donor and acceptor) are positioned in close proximity (20-60 A°). Ruthenium-DNA conjugates emit in the range of 550-750 nm, while osmium complexes exhibit a

MLCT absorption peak at 488 nm with a tail at 580 nm. This provides slight overlap between the donor emission (Ru-complex) and the absorption peak of the acceptor (Os-complex). Thus FRET can occur between $Ru(bpy)_3^{2+}$ and $Os(bpy)_3^{2+}$ when placed in close proximity.[31] The system was designed so the donor (ruthenium complex) is conjugated to DNA building block **2** to obtain building block **3**, where the ruthenium complex becomes an integral part of the square template. The acceptor (osmium complex) can be assembled on one of the single-stranded DNA on building block **1** through canonical base-pairing. Hybridization of building blocks **1** and **3** results in the formation of a square with a ruthenium complex positioned precisely at one of the corners. Addition of metal conjugated strands **39** and **42** results in the positioning of osmium complex in an exact position with respect to the ruthenium complex to afford metal squares **15-16**. It is of note, however that preliminary computational modeling using AMBER force-field calculations of the squares suggests that the ruthenium complex and the osmium complex possess comparable distance in all the squares; thus FRET is expected to be similar for these systems, and was measured only to ascertain correct positioning of the multiple metals. Figure 4.10 shows the steady state emission of the square containing ruthenium and osmium, and table 1 summarizes the emission fraction being quenched using different DNA-osmium conjugates, **39**, **40**, **42** or **43**. The results indicate comparable quenching of 29%-35% for structures **15** – **18** when placing osmium complexes in various positions relative to the Ru complex. However, when DNA-osmium is mixed with **3** in the absence of building block **1** only 15% quenching is observed, this low reduction in emission can be attributed to the intermolecular interaction between ruthenium and osmium conjugates. Preliminary computational modeling was preformed using HyperChem of the square, and the results suggest that the ruthenium complex and the osmium complex to posses similar distance in all systems.

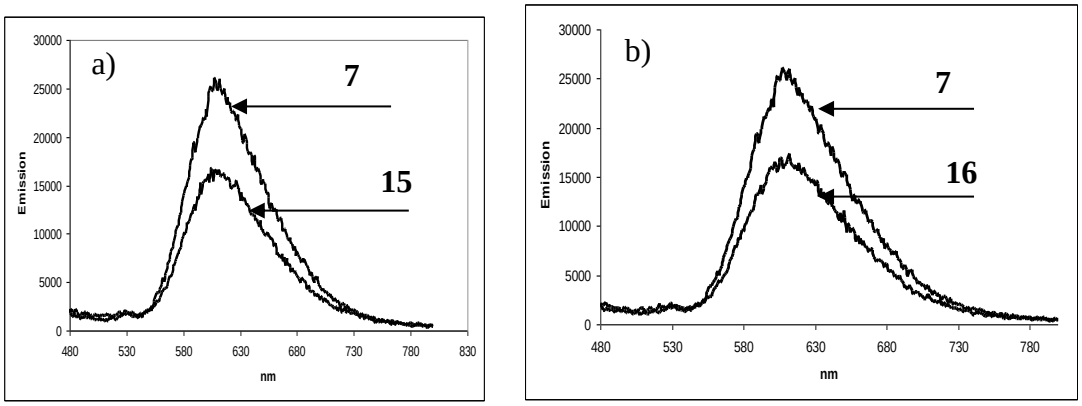

Figure 7. Emission quenching experiments. Steady state emission spectra of **7** and **15** (a), and **7** and **16** (b).

Conclusions

In conclusion, a new DNA nano-square motif has been synthesized from oligonucleotides containing bipyridyl ligands. This DNA discrete square was formed from two easily accessible building blocks. By introducing two complementary single strands on the self assembled structure, functional molecules can be precisely

positioned on the square structure. This methodology is used to assemble hetero-polynuclear metals on this DNA square, where ruthenium and osmium complexes are positioned in a corner of square according to the base pairing of transition metal-DNA conjugates. The metal-DNA assembly is studied using PAGE and FRET experiments. Quenching of the ruthenium emission of up to 35% is obtained as result of the DNA self-assembly. Simply by choosing the right components (number of bases, DNA sequences, site of conjugation, metal ions, and peripheral ligands) we can control the size of the self-assembled DNA, and the distance between the chromophores. This can lead to applications in nanooptics and light-harvesting.

Experimental Section:

General:

4,4-Dimethyl-dipyridyl, bipyridine, trityl chloride, p-anisylchloro-diphenylmethane, bipyridine, ruthenium(III) chloride hydrate, concentrated sulfuric acid, chromium(IV)oxide, selenium oxide, sodum borohydride, sodium metabisulfate, ammonium hexachloroosmate(IV), triethylamine, dimethylaminopyridine, ethylenediaminetetracetic acid (EDTA), magnesium chloride ($MgCl_2.6H_2O$), tris(hydroxymethyl)-aminomethane (Tris), acetic acid, formamide and StainsAll were purchased from Aldrich. 2-Cyanoethyl diisopropylchlorophosphor-amidite, 2-cyanoethyl N,N,N,N-tetraisopropyl phosphane, guanidine derivative 500 Å LCAA-CPG support, cytodine or guanidine derivative 2000 Å LCAA-CPG support, 5-ethylthiotetrazole, dry acetonitrile, DNA phosphoramidite bases and reagents used for automated DNA synthesis were purchased from ChemGenes-Canada.

Instruments and Methods:

c ^{1}H NMR, and ^{13}C NMR spectra were recorded on a varian M400 spectrometer operated at 400.140 MHz. ^{31}P NMR were recorded on a Gemini 200 MHz NMR spectrometer. Matrix assisted laser desorption time-of-flight (MALDI-TOF) spectra of oligonucleotides were recorded using a KOMPACT MALDI III mass spectrometer. UV/vis spectra were recorded on a Varian Cary 300 spectrophotometer. Fluorescence experiments were recorded on a PTI (Photon Technology International) TimeMaster Model C-720F spectrofluorimeter. The slit widths were 6 nm for both excitation and emission. DNA oligonucleotides were synthesized using standard automated oligonucleotide solid-phase synthesis on a Perspective Biosystems Expedite 8900 DNA synthesizer. 20 X 20 cm vertical Hoefer 600 electrophoresis unit was used for the gel electrophoresis experiments.

Synthesis of bipyridine-mono-trityl 21:

4,4’-dihydroxymethylbipyridine (0.146 g, 0.66 mmol), MMT-Cl (0.204 g, 0.66 mmol) and DMAP (0.010 g, 0.08 mmol) were dissolved in dichloromethane (600 ml). To the stirred solution, diisopropylethylamine (0.202 g, 1.98 mmol, 0.278 ml) was

added under nitrogen, and the stirring was continued for six hours. The solvent was removed and the product was purified by column chromatography under basic conditions using silica gel (8.5:1.0:0.5 CH_2Cl_2:Hexanes:Et_3N). The product was obtained in 50% yield. ^{1}H NMR (400 MHz, CD_3CN); δ 8.63 (d, 1H, bpy-*H*), 8.56 (d, 1H, bpy-*H*), 8.32 (s, 1H, bpy-*H*), 8.22 (d, 1H, bpy-*H*), 7.56 (d, 1H, Ar), 7.51 (d, 4H, Ar), 7.38 (d, 2H, Ar), 7.30 (m, 5H, Ar), 7.23 (m, 2H, Ar), 6.83 (d, 2H, Ar), 4.75 (s, br, 2H, C*H*$_2$), 4.29 (s, 2H, C*H*$_2$), 4.78 (s, 3H, C*H*$_3$). ^{13}C NMR (400 MHz, CD_2Cl_2); δ 158.92, 155.89, 155.75, 152.21, 149.60, 149.10, 144.44, 135.31, 130.43, 128.35, 128.09, 127.17, 121.72, 121.34, 119.13, 118.57, 113.33, 87.14, 64.64, 63.00, 55.26. The HRMS (M^+) for **4.21** was calculated 486.60, and it was found experimentally 486.23.

Synthesis of the bipyridine-amidite 19:
The mono-protected bipyridine (0.16 g, 0.33 mmol), diisopropylethylamine (0.16 g, 1.33 mmol) and DMAP (0.010 g, 0.08 mmol) were dissolved in dry dichloromethane (15 ml), to this was added 2-Cyanoethyl diisopropylchlorophosphor-amidite (0.30g, 1.98 mmol). The reaction was stirred for three hours under nitrogen. The product was purified by column chromatography using silica gel under basic conditions (65:30:5 CH_2Cl_2:Hexanes:Et_3N). The product was obtained in 95% yield. ^{1}H NMR (400 MHz, CDCl); δ 8.65 (d, 1H, bpy-*H*), 8.60 (d, 1H, bpy-*H*), 8.33 (s, 1H, bpy-*H*), 8.24 (s, 1H, bpy-*H*), 7.52 (m, 5H, Ar), 7.38 (d, 2H, Ar), 7.32 (m, 5H, Ar), 7.23 (d, 2H, Ar), 6.84 (d, 2H, Ar), 4.82 (m, 2H, C*H*$_2$), 4.26 (s, 2H, C*H*$_2$), 3.94 (m, 2H, C*H*$_2$), 3.78 (s, 3H, OC*H*$_3$), 3.66 (s, 2H, C*H*$_2$), 2,68 (m, 2H, NC*H*), 1.23 (m, 12, C*H*$_3$). ^{31}P NMR (200 MHz, CDCl); δ 149.56. ^{13}C NMR (400 MHz, CDCl); δ 158.81, 156.17, 155.80, 149.25, 149.48, 149.45, 144.33, 135.46, 130.52, 128.50, 128.15, 127.25, 121.80, 121.58, 119.11, 118.91, 117.78, 113.45, 109.99, 87.26, 64.90, 64.40, 64.23, 59.04, 58.84, 58.49, 55.61, 55.57, 45.71, 45.64, 43.71, 43.58, 25.13, 25.05, 23.43, 23.32, 20.82, 20.51. The HRMS (M^+) for **19** was calculated 688.76, and it was found experimentally 688.39.

Synthesis of 4'-Methyl-2,2'-bipyridine-4-carboxaldehyde: 4,4'-Dimethyl-2,2'-bipyridine (5.27 g, 28.6 mmol) and selenium oxide (SeO_2) (3.48 g, 31.4 mmol) were suspended in 1,4-dioxane (260 ml), the reaction mixture was refluxed for 24 hours. The solution was filtered while hot. The cooled filtrate was left at room temperature for 3 hours and was filtered again to remove any brown solid. The solvent was removed under vacuum, and the residue was dissolved in ethyl acetate (500 ml), the undissolved solid was removed by filtration, then the filtrate was extracted with sodium carbonate Na_2CO_3 1.0 M (200 ml) to remove any formed carboxylic acids. Then the organic layer was extracted with sodium metabisulfate 0.3 M (3 X 100 ml) to form the aldehyde bisulfate complex. The aldehyde was released from the combined aqueous layers by adjusting the pH to 10 using solid Na_2CO_3 then the product was extracted using dichloromethane (4 X 100 ml), the combined organic

layers were dried under magnesium sulfate. Removing the solvent afforded the aldehyde as white solid in 40% yield (2.24 g, 11.20 mmol). R_f = 0.35 (netural alumina, toluene:ethyl acetate 1:1). ^{1}H NMR (300 MHz, CDCl); δ 10.16 (s, 1H, C*H*O), 8.87 (d, 1H, Ar), 8.84 (s, 1H, Ar), 8.55 (d, 1H, Ar), 8.27 (s, 1H, Ar), 7.71 (d, 1H, Ar), 7.17 (d, 1H, Ar). 2.45 (s, 3H, CH_3). ^{13}C NMR (300 MHz, CDCl); δ 192.00, 158.10, 154.65, 150.58, 149.09, 142.87, 136.10, 125.72, 122.47, 121.77, 120.92, 21.53. The HRMS (M^+) for the desired product was calculated 198.20, and it was found experimentally 198.07.

Synthesis of 4'-Methyl-4-(hydroxymethyl)-2,2'-bipyridine 26: The aldehyde (500 mg, 2.52 mmol) was dissolved in dichloromethane (50.0 ml), the flask was cooled to 0 ^{0}C. To the cooled solution was added sodium borohydride (500 mg, 13.21 mmol) dissolved in aqueous sodium hydroxide solution (5 ml). After completing the addition, the reaction mixture was left to warm to room temperature and continued stirring for another 3 hours. The aqueous layer was extracted with dichloromethane (2 X 100), and the combined organic layers were washed with brain and water, then it was dried under sodium sulfate. The solvent was removed to give the alcohol as white solid (73% yield). ^{1}H NMR (400 MHz, CDCl); δ 8.52 (d, 1H, Ar), 8.44 (d, 1H, Ar), 8.25 (s, 1H, Ar), 8.13 (s, 1H, Ar), 7.23 (dd, 1H, Ar), 7.10 (d, 1H, Ar), 4.71 (s, 2H, CH_2) 4.59 (s, br, 1H, O*H*), 2.39 (s, 3H, CH_3). ^{13}C NMR (400 MHz, CDCl); δ 155.73, 155.58, 151.87, 149.05, 148.70, 148.60, 124.86, 122.40, 121.22, 118.75, 63.13, 21.21. The HRMS (M^+) for **26** was calculated 199.11, and it was found experimentally 199.09.

Synthesis of [4'-Methyl-4-(hydroxymethyl)-2,2'-bipyridine]bis(2,2'-bipyridine)ruthenium Hexafluorophosphate, {Ru^{II}(4-CH_2OH-4'-Mebpy)(bpy)$_2$}(PF_6)$_2$ 29:

A solution of Ru(bpy)$_2$Cl$_2$ (0.140 g, 0.29 mmol) and 4'-methyl-4-(hydroxymethyl)-2,2'-bipyridine (0.058 g, 0.29 mol) in 1:1 ethanol:water (15 ml) was stirred and refluxed for 12 hrs. The solvent was removed under reduced vacuum, and the solid was dissolved in water. Addition of ammonium hexafluorophosphate solution (excess) resulted in the precipitation of the red-orange product. The complex was collected by filtration, washed with water and ether to give 85% yield, (0.222 g, 0.24 mmol). ^{1}H NMR (300 MHz, CD_3CN); δ 8.49 (s, 2H, Ar), 8.46 (s, 3H, Ar), 8.39 (s, 1H, Ar), 7.58 (t, 4H, Ar), 7.66 (br, 4H, Ar), 7.53 (d, 1H, Ar), 7.45 (d, 1H, Ar), 7.30 (m, 5H, Ar), 7.17 (d, 1H, Ar), 4.88 (s, 2H, CH_2), 3.78 (br, 1H, O*H*), 2.62 (s, 3H, CH_3). The HRMS (M^+) for **29** was calculated 903.60, and it was found experimentally 904.06.

Synthesis of Os(bpy)$_2$Cl$_2$ 28:

This complex was synthesized according to a published procedure.[33b] A mixture of $(NH_4)_2[OsCl_6]$ (0.50 g, 1.1 mmol), 2,2'-bipyridine (0.43 g, 2.2 mmol), and 1,2-

ethyleneglycol (18 ml) was stirred and refluxed under nitrogen for two hours. The cooled reaction mixture was treated with $Na_2S_2O_4$ (1M, 30 ml) to reduce any Os(III) that might have formed during the reaction. After standing over night at 0 °C, the black precipitate was collected using vacuum filtration. The solid was washed with water and diethyl ether. The reaction yield was 70%. The complex was used for the next step without further purification.

Synthesis of [4'-Methyl-4-(hydroxymethyl)-2,2'-bipyridine]bis(2,2'-bipyridine)osmium Hexafluorophosphate, $\{Os^{II}(4\text{-}CH_2OH\text{-}4'\text{-}Mebpy)(bpy)_2\}(PF_6)_2$ 30:[33b]

A mixture of $Os(bpy)_2Cl_2$ (0.164 g, 0.29 mmol), 4'-methyl-4-(hydroxymethyl)-2,2'-bipyridine (0.050 g, 0.29 mmol), and Na_2HPO_4 (0.10 g) in 1:1 ethanol:water (15 ml) was refluxed and stirred for 12 hrs. The solvent was reduced to 5 ml, addition of concentrated NH_4PF_6 (excess) resulted in the precipitation of dark brown solid. ^{1}HNMR (300 MHz, CD_3CN); δ 8.49 (s, 2H, Ar), 8.46 (s, 3H, Ar), 8.39 (s, 1H, Ar), 7.58 (t, 4H, Ar), 7.66 (br, 4H, Ar), 7.53 (d, 1H, Ar), 7.45 (d, 1H, Ar), 7.30 (m, 5H, Ar), 7.17 (d, 1H, Ar), 4.88 (s, 2H, C*H*$_2$), 3.78 (br, 1H, O*H*), 2.62 (s, 3H, C*H*$_3$). The HRMS (M^+) for **30** was calculated 992.76, and it was found experimentally 994.12. The complex was collected using filtration, and was washed with cooled water and ether to give (0.258 g, 0.26 mmol) in 90% yield.

General procedure for the synthesis of DNA-bpy 1 and **2:**

The vertex, amidite derivative of bpy, was dissolved in anhydrous acetonitrile to get a concentration of (0.5 μM) and placed in the automated DNA synthesizer. This monomer was used during the DNA synthesis in similar way as the conventional DNA phosophoramidite reagent with extending the coupling and deprotection steps to 5 and 2 minutes respectively. Each bpy-DNA conjugate was grown on 500 Å LCAA-CPG solid support, after building the desired number of sequences, the final DMT group was removed. The oligonucleotide was cleaved from the solid support and the DNA-bases were deprotected using concentrated ammonium hydroxide at 55 °C. The solvent was removed and the product was purified using 24% TBE denaturing polyacrylamide gel, the bands containing the desired product were visualized using UV lamp and quickly excised, crushed and extracted into 6 ml of water (16 hours, 50 °C). The resulting solution was concentrated to 1 ml, and the product was desalted using sephadex G-25 size exclusion chromatography. DNA was quantified by UV-vis spectroscopy, concentration was calacualted using Beer's law $A_{total} = A_{vertex} + A_{DNA}$, the extinction coefficient for the bpy at 260 nm was calculated to be 5800 L. mol^{-1}. cm^{-1}. The synthesized oligonucleotides **1** and **2** were characterized using matrix assisted laser desorption ionization time-of-flight (MALDI-TOF) mass spectroscopy, table 1 shows the sequences, and reports the theoretically calculated and the experimentally obtained values for molecular weights. The purity of the isolated DNA was confirmed using 24% PAGE (See Figure 1).

Table 1. Obtained MALDI-TOF mass spectroscopy for **1** and **2**

Sequences (5`-3`)	Calculated	Obtained
GCACGAGTbpyCCTAACGCbpyCGGTA TCAbpyGGCTTACG	[M] 10641	[M+Na] 10664
ACTCGTGCbpyCGTAAGCC	[M] 5117.03	[M] 5117.62

General procedure for the synthesis of DNA-Metal complex conjugates:

The DNA strand was first synthesized on a 1 μM scale on 1000 Å CPG. Conjugation of metal complex was accomplished using a reverse coupling technique. The hydroxyl group of the last base on the DNA strand was deprotected on the DNA synthesizer, the column was removed from the machine and fitted with two plastic syringes; one syringe was charged with dry tetrazole activator solution (200 μL, 0.5 M) and the second syringe was charged with 2-(cyanoethyl)-tetraisopropylphosphodiamidite (200 μL).

The two solutions were mixed manually through the column. The phosphitylation was allowed to take place for 4 hours by placing the column equipped with two syringes on a shaker.

The syringes and the solvent were quickly removed and the column was placed on the DNA machine and washed with dry acetonitrile.

The next step was to conjugate the metal complex to the activated DNA strand, this was accomplished again manually using off column techniques. Again, the column was removed from the machine and fitted with two plastic syringes; one syringe was charged with dry ethyl-thiotetrazole activator solution (200 μL, 0.5 M) and the second syringe was charged with a dry solution of metal complex (5 mg in 200 μL) in acetonitrile. The two solutions were mixed manually through the column. The reaction was left overnight. The reagents were removed and the column was rinsed with dry acetonitrile on the DNA machine. Finally the solid support containing DNA was treated with a capping solution to protect any unreacted hydroxyl group on DNA, and then treated with oxidizing reagent. The DNA was cleaved from the solid support using concentrated ammonium hydroxide at 50 °C for one hour. The bases were deprotected using concentrated ammonium hydroxide at 50 °C for overnight. Metal-DNA conjugate was purified by denaturing 25% PAGE. Bands corresponding to the conjugated molecule were excised. The desired product could be visualized using UV lamp and could be seen by naked eyes as orange-green and green-brown for ruthenium and osmium conjugates respectively. The gel pieces were crushed and the DNA conjugate was extracted using water (6 ml) at 55 °C for overnight. Using 25G sephadex, the salts was removed to afford pure conjugates as analyzed using by PAGE and MALDI-TOF.

Table 2. Obtained MALDI-TOF mass spectroscopy for **3** and **38-43**

Metal-DNA conjugate	Calculated	Obtained
3	6096.57	[M-3H] 6093.31
38	3082.43	[M] 3084.67
39	3171.19	[M] 3171.56
40	3171.19	[M+4H] 3175.85
41	3139.93	[M+H] 3140.32
42	3227.19	[M] 3227.07
43	3227.19	[M] 3227.87

Enzymatic digestion:

Mung Bean Nuclease (MBN) was used to test for whether the structure obtained from the hybridization of **1** and **2** is cyclic or linear. MBN is used to selectively digest single strand DNA while leaving double stranded DNA intact. For this reason the enzymatic activity of MBN was optimized for the bipyridine-DNA conjugates **1** and **2**. It was found that 30 unites of MBN (at 5 °C for 3 hours) can completely digest single stranded DNA **1** and while the double stranded DNA can not be digested. The reaction was performed at low temperature to prevent annealing. Final concentration of DNA (13 μM) was prepared in buffer [TAE.Mg (12.5 mM Mg^{2+})], to this was added 30 unites of enzyme. The mixture was incubated in fridge for three hours. The reaction products were analyzed using a 16% native PAGE gel. The bands on the developed gel were visualized using stainsall and scanned using computer scanner. Figure 4.4 shows the result of the MBN digesting experiment and clearly shows the digestion of the single DNA strand and while **8** remain stable at the same conditions. The results indicate that the structure nature of **8** is cyclic.

Hybridization Experiments

For the hybridization all samples were prepared in TAE buffer (about 0.02 O.D in 7 μL), the DNA building blocks were added sequentially at <10 °C, the mixture was left to incubate for at least 20 minutes before the following addition. Cooled loading buffer (7 μL), and glycerol in TAE buffer, were added. Samples were loaded on 16% nondenaturing gels placed in 20 X 20 cm vertical Hoefer 600 electrophoresis unit. The gel was developed using TAE buffer system at 70-80 V for 14-15 hours in the fridge. Developed gel was stained using stains all and scanned.

Fluorescence Experiments:

Fluorescence emission spectra were collected on a PTI (Photon Technology International) TimeMaster Model C-720F spectrofluorimeter. Microsize quartz cuvette was used for all experiments. All samples were purged with high purity nitrogen gas prior to running the experiments. Excitation wavelength was adjusted at 450 nm and the emission was collected from 580nm to 750 nm, the bandwidth was

fixed at 6 nm for both the excitation and the luminescence lights. For quenching experiments, the assembled structures were preserved at < 10 °C. Quenching efficiency was calculated by the following equation: Q% = I_0-I/ I_0 X 100, where I_0 and I are the integrated areas of the emission of ruthenium complex alone and in the presence of DNA-osmium conjugate respectively.

References:

1- a) Balzani, V.; Juris, A.; Venturi, M., *Chem. Rev.*, **1996**, *96*, 759-833. b) Ajay Kumar Manna, *International Journal of Science and Research*, **2015**, *5*, 892-899. c) Schlichthaerle, T.; Strauss, M. T.; Schueder F.; Woehrstein, J. B.; Jungmann, R., *Current Opinion Biotechnology*, **2016**, *39*, 41-47. d) Veneziano, R.; Ratanalert, S.; Zhang, K.; Zhang, F.; Yan, H.; Chiu, W.; Bathe, M., Science, **352**, 1534.

2- a) De Cola, L.; Belser, P. *Coord. Chem. Rev.*, **1998**, *177*, 301-346. b) Kondo, J.; Tada, Y.; Dairaku, T.; Hattori, Y.; Saneyoshi, H.; Ono, A.; Tanaka, Y., *Nature Chemistry*, **2017**, 456-463.

3- Ward, M. D.; Barigelletti, F., *Coord. Chem. Rev.*, **2001**, *216-217*, 127-154

4- Moser, C. C.; Keske, J. M.; Warncke, K.; arid, R. S.; Dutton, P. L., *Nature*, **1992**, *355*, 796-802.

5- McDermott, G.; Prince, S. M.; Freer, A. A.; Hawthrornthwaite-Lawless, A. M.; Papiz, M. Z.; Cogdell, R. J.; Isaacs, N W. *Nature*, **1995**, *374*, 517-521

6- Beyeler, A.; Belser, P., *Coord. Chem. Rev.* **2002**, *230*, 29-39

7- Ballardini, R.; Balzani, V.; Credi, A.; Gandolfi, M. T.; Venturi, M., *Acc. Chem. Res.*, **2001**, *34*, 445-455

8- Dürr, H.; Bossmann, S., *Acc. Chem. Res.*, **2001**, *34*, 905-917

9- Schubert, U. S.; Eschbaumer, C., *Angew. Chem. Int. Ed.* **2002**, *41*, 2892-2926

10- a) Holder, E.; Langeveld, B. M. W.; Schubert, U. S. *Adv. Mater.* **2005**, *17*, 1109-1121. b) Tor, Y. *Chimie*, **2003**, *6*, 755-766. c) Venturi, M.; Credi, A.; Balzani, V. *Coord. Chem. Rev.* **1999**, *185-186*, 233-256. d) Holiday, B. J.; Mirkin, C. A. *Angew. Chem. Int. Ed.* **2001**, *40*, 2022-2043. e) Sun,S.-S.; Lees, A. J. *Coord. Chem. Rev.* **2002**, *230*, 171-192. f) Beer, P. D.; Szemes, F.; Balzani, V.; Sala, C. M.; Drew, M. G. B.; Dent, S. W.; Maestri, M. *J. Am. Chem. Soc.*, **1997**, *119*, 11864-11875. g) Bassani, D. M.; Lehn, J.-M.; Serrni, S.; Puntoriero, F.; Campagna, S. *Chem. Eur. J.*, **2003**, *9*, 5936-5946. h) De Cola, L.; Belser, P.; von Zelewsky, A.; Vögtle, F. *Coord. Chem. Rev.* **2007**, *360*, 775-784. i) Venturi, M.; Marchioni, F.; Ribera, B. F.; Balzani, V.; Opris, D. M.; Schluter, A. D., *ChemPhysChem*, **2006**, *7*, 229-239. j) Ward, M. D.; Barigelletti, F., *Coord. Chem. Rev.*, **2001**, *216-217*, 127-154.

11- a) Feldkamp, U.; Niemeyer, C. M. *Angew. Chem. Int. Ed.* **2006**, *45*, 1856-1876. b) Rosi, N. L.; Mirkin, C. A. *Chem. Rev.* **2005**, *105*, 1547-1562

12- Lawrence, D. S.; Jiang, T.; Levett, M. *Chem. Rev.* **1995**, *95*, 2229-2260

13- Whitesides, G. M.; Gryzbowski, B. *Science*, **2002** *295*, 2418-2421

14- Lehn, J. M. *Science*, **2002** *295*, 2400-2403
15- Steed, J. W.; Atwood, J. L. *Supramolecular Chemistry*; Wiley: N.Y., 2000.
16- Seeman, N. C., *Nature*, **2003,** *421*, 427-431
17- Wengel, J., *Organic & Biomolecular Chemistry*, **2004**, *2*, 277-280
18- Lin, C.; Liu, Y.; Rinker, S.;Yan, H., *ChemPhysChem*, **2006**, *7*, 1641-1647
19- a) LaBean, T. H.; Li, H., *Nano Today*, **2007**, *2*, 26-35. b) Pak, S. H.; Yin, P.; Liu, Y.; Reif, J. H.; LaBean, T. H.; Yan, H. *Nano. Lett.* **2005**, *5*, 729-733.
20- Yan, H.; Park, S. H. Ginkelstein, G.; Reif, J. H.; LaBean, T. H. *Science* **2003**, *301*, 1882
21- Niemeyer, C. M. *Angew. Chem. Int. Ed.* **2001**, *40*, 4128-4158
22- Aldaye, F. A.; Sleiman. H. F. *J. Am. Chem. Soc.* **2007**, *129*, 4130-4131
23- Aldaye, F. A.; Sleiman. H. F. *Angew. Chem. Int. Ed.* **2006**, *45*, 2204-2209
24- Pinto, Y.; Le, J. D.; Seeman, N. C. ; Musier-Forsyth, K. ; Taton, T. A.; Kiehl, R. A. *Nano. Lett.* **2005**, *5*, 2399-2402. b) Zheng, J.; Constantinou, P. E.; Micheel, C.; Alivisatos, P. A.; Kiehl, R. A.; Seeman, N. C. *Nano. Lett.* **2006**, *6*, 1502-1504.
25- Zhang, J.; Liu, Y.; Ke, Y.; Yan, H. *Nano. Lett.* **2006**, *6*, 248-251.
26- Gothelf, K. V.; LaBean, T. H. *Org. Biomol. Chem.* **2005**, *3*, 4023-4037
27- Mitra, D.; Di Cesare, N.; Sleiman, H. F. *Angew. Chem. Int. Ed.* **2004**, *43*, 5804-5808
28- Stewart, K. M.; Rojo, J.; McLaughlin, L. W. *Angew. Chem. Int. Ed.* **2004**, *43*, 5808-5811
29- Wiederholt, K.; McLaughlin, L. W. *Nucleic Acids Res.*, **1999**, *27*, 2487-2493
30- Stewart, K. M.; McLaughlin, L. W. *J. Am. Chem. Soc.* **2004**, *126*, 2050-2057
31- Stewart, K. M.; McLaughlin, L. W., *Chem. Commun.* **2003**, 2934
32- Czlapinsxi, J. L.; Sheppard, T. L., *J. Am. Chem. Soc.* **2001**, *123*, 8618-8619
33- a) Fleming, C. N.; Dupray, L. M.; Papanikolas, J. M.; Meyer, T. J. *J. Phys. Chem. A*, **2002**, *106*, 2328-2334. b) Younathan, J. N.; McClanahan, S. F.; Meyer, T. J. *Macromolecules*, **1989**, *22*, 1048-1054. c) worl, L. A.; Strouse, G. F.; Younathan, J. N.; Baxter, S. M.; Meyer, T. J. *J. Am. Chem. Soc.* **1990,** *112*, 7571-7578. d) Fleming, C. N.; Maxwell, K. A.; Desimone, J. M.; Meyer, T. J.; Papanikolas, J. M. *J. Am. Chem. Soc.* **2001,** *123*, 10336-10347. and references there in.
34- Newkome, G. R.; He, E.; Moorefield, C. N., *Chem. Rev.*, **1999**, *99*, 1689-1746
35- a) Ward, M. D.; Barigelletti, F., *Coord. Chem. Rev.*, **2001**, *216-217*, 127-154. b) Claire, M. W. ; Gonzaler, M. F.; Bardwell, D. A.; Rees, L. H.; Jeffery, J. C.; Ward, M. D.; Armaroli, N.; Calogero, G.; Barigelletti, F. *J. Chem. Soc. Dalton. Trans.* **1997**, 727-735. c) Armaroli, N.; Barigelletti, F.; Calogero, G.; Flamigni, L.; Claire, M. W. ; Ward, M. D. *Chem. Commun.*, **1997**, 2181-2182.

36- a) Holmlin, R. E.; Tong, R. T.; Barton, J. K., *J. Am. Chem. Soc.* **1998**, *120*, 9724-9725. b) Erkkila, K. E.; Odom, D. T.; Barton, J. K. *Chem. Rev.*, **1999**, *99*, 2777-2795.
37- Bicenkova, E. V.; Yu, X.; Bhadra, P.; Heissigerova, H.; Pope, S. J. A.; Coe, B. J.; Faulkner, S.; Douglas, K. T., *Inorg. Chem.* **2005**, *44*, 4112-4114
38- Hurley, D.; Tor, Y., *J. Am. Chem. Soc.* **1998**, *120*, 2194-2195
39- Holmlin, R. E.; Tong, R. T.; Barton, J. K., *J. Am. Chem. Soc.* **1998**, *120*, 9724-9725
40- a) Hurley, D. J.; Tor, Y., *J. Am. Chem. Soc.* **2002**, *124*, 3749-3762. b) Hurley, D. J.; Tor, Y., *J. Am. Chem. Soc.* **2002**, *124*, 13231-13231
41- Miao, R.; Brewer, K. J., *Inorg. Chem Chem. Commun.* **2007**, *10*, 307-312
42- Gianolio, D. A.; Segismundo, J. M.; Mclaughlin, L. W. *Nucleic Acids Res.* **2000**, *28*, 2128-2134.
43- Fukolka, F.; Schoeps, O.; Woggon, U.; Niemeyer, C. M. *Bioconjugate Chem.* **2007**, *18*, 621-627.
44- Miyoshi, D.; Karimata, H.; Wang Z.-M.; Koumoto, K.; Sugimoto, N. *J. Am. Chem. Soc.* **2007**, *129*, 5919-5925

الملخص:

في هذه الدراسة قمنا بتصميم و تشكيل مربعات في حجم النانو متكونه من الحامض الريبوزي النووي منقوص الاكسجين DNA. تصميم هذه المربعات يمكن استخدامه في عمليه تثبيت و تموضع معقدات الروثينيوم و الاوزميوم في زوايا المربع. الاستراتيجية المتبعة في هذه الطريقة مبنية علي وجود شريط DNA احادي في احد اضلاع المربع. مما يمكن المعقدات المرتبط بشريط DNA الموافق للموجود علي المربع بتكوين مزدوج DNA مما يؤدي الي تموضع المعقد في مكان محدد من المربع.

بهذه الطريقة تمكنا من تكوين اشكال مربعه تحمل معقدات متعددة في حجم النانو، حيث يكون معقدات الروثينيوم و الاوزميوم موجوده في مسافات محدده و اتجاهات مقننه حسب التسلسل DNA. هذه الاجسام النانويه تم اثبات تكوينها و تركيبها باستخدام طرق الفصل الكروماتوغرافي، و دراسه اطفاء وميض luminescence المعقدات. هذه الاستراتيجية تمكن من تموضع المعقدات و المركبات في اشكال مختلفة و بمسافات مختلفة تبعا لنوع و عدد الاحماض النووية المستخدمة في DNA. هذه الطريقة من الممكن ان تؤدي الي تطبيقات في مجال النانواوبتيك، البناء الضوئي الصناعي، و مجالات التشخيص الطبي.